Chapter 12
Dam-Operation Policy During Hurricane Season Using Regional Flows with Canonical Correlation Analysis

Juan Pablo Molina-Aguilar, Alfonso Gutierrez-López, and Ivonne Cruz Paz

Abstract The period of hurricanes extends along the Mexican coast from May to October and year after year causes considerable economic and human damage. An important part of risk management during a disaster of this type is the operation of dams. Many of these structures are used for water supply and electric-power generation; however, their maximum flow-control capacity is of great importance for flood-risk management.

The hydrometric data of 15 stations located within the basin of the El Caracol dam are used. Maximum precipitation data are also used in 27 stations within the basin. Note that the series used contain data for years with hurricane records. With these data, a regional frequency analysis is performed using the Gradex approach, which highlights the impact of precipitation from hurricane events.

Using a matrix of physiographic, climatological, and environmental basin characteristics, in addition to the characteristics of the reservoir and the operation of the dam, a principal component analysis EOF is performed to prioritize the variables that must be included in the operation policy of the dam. With the satellite images recorded every 15 min, the precipitation intensities of the hurricanes are calculated using the hydro-estimator technique and correlated with the flow rates measured by performing a canonical correlation analysis. The results show that downscaling between the precipitation data coming from the satellite images and the measured flow rates on the surface, it is possible to propose a policy for the supply and control operation of dams. The conclusion is that the hydro-estimator techniques together with the canonical correlation analysis are adequate procedures to propose the operation policies in dams during the hurricane season.

Keywords Hurricanes · Dam operation · Principal component analysis · Canonical correlation analysis

J. P. Molina-Aguilar · A. Gutierrez-López (✉) · I. C. Paz
Universidad Autonoma de Queretaro, Water Research Center, Centro de Investigaciones del Agua-Queretaro (CIAQ), International Flood Initiative, Latin-American and the Caribbean Region (IFI-LAC), International Hydrological Programme (IHP-UNESCO), Queretaro, Mexico
e-mail: alfonso.gutierrez@uaq.mx

J. A. Raynal-Villasenor (ed.), *Water Resources of Mexico*, World Water Resources 6,
https://doi.org/10.1007/978-3-030-40686-8_12

12.1 Introduction

In Mexico, there are approximately 5000 dams that are administered by the National Water Commission (Comision Nacional del Agua); the Federal Electricity Commission (CFE); the International Boundary and Water Commission (CILA), Section Mexico; Associations of Users and Private Owners; representatives of state, municipal and Mexico City governments, as well as formal and informal users.

Therefore, it is necessary to have an Emergency Action Plan (EAP) where all the institutions, government sectors and users mentioned above, must collaborate in implementing, in a coordinated way, the necessary actions to perform an evacuation procedures and/or make a warning alert in case of an emergency. This would help to avoid and/or to reduce the loss of human lives and goods and/or environmental damage in the geographical environment of the dams that are already rated as high risk with formal classification with high damage potential. For dams classified as high risk or with a high damage potential in the event of failure, the responsible entity must perform a periodic or intermediate safety inspection every year (see NMX-AA-175/2-SCFI-2016 Safe operation of dams. 2. Security inspections) and inform the the National Water Commission (Comision Nacional del Agua).

Meanwhile, for the diversion dams, storage dams or flood control dams with dam bodies with heights above the river channel less than 15 m and with a capacity to the Ordinary High Water Level (NAMO) less than 250,000 cubic meters, and that are classified preliminarily at low risk or whose formal classification of consequences for their potential for damage in case of failure it is low (see NMX-AA-175-SCFI-2015 Safe operation of dams, Part 1.- Risk analysis and classification of dams), they do not require the preparation of an EAP. Instead, they should only have a directory of the local, state, or federal authorities to inform them that the dam is in a state of emergency.

In all these cases, the dams need to have an adequate operating policy, especially for flood control in the hurricane season.

The period of hurricanes extends along the Mexican coasts from May to October, and year after year hurricane causes significant economic and human losses. An important part of risk management during a disaster of this type is the adequate operation of dams. Many of these structures are used for water supply and electric-power generation; however, their maximum flow-control capacity is of great importance for flood-risk management.

To collect rainfall and other hydrometric data, Mexico has about little more than 5000 weather stations and 1000 flow measurement sites. So, it is very useful to have real-time predictions of precipitation during the hurricane season. Thus, the hydro-estimator technique is used to correlate the operation policies of the dams with the trajectory and intensity of hurricane precipitation.

Note that the series used contain data from years with hurricane records. With these data, a regional frequency analysis is performed using the Gradex approach, which highlights the impact of precipitation from hurricane events. Using a matrix of physiographic, climatological, and environmental basin characteristics, in addition to the characteristics of the reservoir and the operation of the dam, a canonical correlation analysis is performed to prioritize the variables that must be included in the operation policy of the dam.

With satellite images recorded every 15 min, the precipitation intensities of the hurricanes are calculated using the hydro-estimator technique and correlated with the flow rates measured through a process named canonical correlation analysis.

The results show that the downscaling between the precipitation coming from satellite images and measured flow rates on the surface is possible to propose a policy of operation for the supply and control dams. The conclusions are intended to establish the technique of hydro-estimator in combination with canonical correlation analysis as an appropriate procedure to propose dam operation policies during the hurricane season.

12.2 Theoretical Framework

12.2.1 Canonical Correlation Analysis

The canonical correlation analysis can be considered as the logical generalization of the multiple regression analysis whose objective is the simultaneous correlation of p-dependent variables with respect to q-independent variables, establishing the linear combination of both sets of variables, through random vectors that maximize the value of the correlation coefficient (Hair et al. 2009). Considering the two sets of variables involved in the development of hydro-meteorological phenomenon, the first of which groups the independent variables $X = (x_1, x_2, \ldots, x_p)$ and in the second the dependent variables are grouped $Y = (y_1, y_2, \ldots, y_q)$ through V and W that are two compound lineal variables, which are named canonical variables (Crespin 2016).

These canonical variables are the product of the linear combination by multiplying the transpose of the weight vectors a and b by the set of dependent variables s and independent variables s, respectively.

$$V = a^T X = \left(a_1, a_2, \ldots, a_p\right) \begin{pmatrix} x_1 \\ x_2 \\ \cdot \\ x_p \end{pmatrix} = a_1 x_1 + a_2 x_2 + \ldots + a_p x_p \tag{12.1}$$

$$W = b^T Y = \left(b_1, b_2, \ldots, b_q\right) \begin{pmatrix} y_1 \\ y_2 \\ \cdot \\ y_q \end{pmatrix} = b_1 y_1 + b_2 y_2 + \ldots + b_q y_q \tag{12.2}$$

To do this, the sample covariance matrix of size p x q for the first and second set of variables is defined as

$$C = \begin{pmatrix} C_{XX} & C_{XY} \\ C_{YX} & C_{YY} \end{pmatrix} \tag{12.3}$$

where

$$C_{YX} = {C_{XY}}^{T} \tag{12.4}$$

Similarly, the canonical correlation between both composite variables is defined as

$$corr(V, W) = \frac{\mathrm{cov}(V, W)}{\sqrt{\mathrm{var}(V)}\sqrt{\mathrm{var}(W)}} = \frac{a^{T} C_{XY} b}{\sqrt{a^{T} C_{XX} a}\sqrt{b^{T} C_{YY} b}} \tag{12.5}$$

Defining as restrictions of the problem that

$$Var(V) = a^{T} C_{XX} a = 1 \tag{12.6}$$

$$Var(W) = b^{T} C_{YY} b = 1 \tag{12.7}$$

So, the problem of canonical correlation is reduced to maximize

$$Corr(V, W) = a^{T} C_{XY} b \tag{12.8}$$

To realize the maximization of the canonical correlation, a Lagrange function of two parameters, τ_1 and τ_2, is defined as

$$L(a, b) = a^{T} C_{XY} b - \tau_1 \left(a^{T} C_{XX} a - 1 \right) - \tau_2 \left(b^{T} C_{YY} b - 1 \right) \tag{12.9}$$

From which, we obtain the partial derivatives of the Lagrange function in terms of the weight vectors solution *a* and *b*.

$$\frac{\partial L(a, b)}{\partial a} = C_{XY} b - 2\tau_1 C_{XX} a = 0 \tag{12.10}$$

$$\frac{\partial L(a, b)}{\partial b} = C_{XY}^{T} a - 2\tau_2 C_{YY} b = 0 \tag{12.11}$$

Both partial derivatives make a possible construction of a system of equations that enable us to determine the unknown vectors.

$$C_{XY}b = 2\tau_1 C_{XX}a \tag{12.12}$$

$$C_{XY}^T a = 2\tau_2 C_{YY}b \tag{12.13}$$

According to Eqs. (12.6) and (12.7), proceed to multiply Eqs. (12.12) and (12.13) by the transposed vectors to respect the initial approach.

$$\begin{gathered}
(C_{XY}b = 2\tau_1 C_{XX}a)a^T \\
a^T C_{XY}b = 2\tau_1 a^T C_{XX}a \\
a^T C_{XY}b = 2\tau_1 \\
\left(C_{XY}^T a = 2\tau_2 C_{YY}b\right)b^T \\
b^T C_{XY}^T a = 2\tau_2 b^T C_{YY}b
\end{gathered} \tag{12.14}$$

$$b^T C_{XY}^T a = 2\tau_2 \tag{12.15}$$

Developing the left side of Eqs. (12.14) and (12.15) yields a scalar pattern and because

$$\left(a^T C_{XY}b\right)^T = b^T C_{XY}^T a = 1, \tag{12.16}$$

both equations are equivalent as defined by $\lambda = 2\tau_1 = 2\tau_2$. Therefore, we can rewrite Eqs. (12.12) and (12.13) as

$$C_{XY}b = \lambda C_{XX}a \tag{12.17}$$

$$C_{XY}^T a = \lambda C_{YY}b \tag{12.18}$$

This allows reduction of the system using the method of algebraic substitution clearing the vector a of Eq. (12.17) to substitute in Eq. (12.18)

$$\begin{gathered}
C_{XY}^T \left[\frac{1}{\lambda} C_{XX}^{-1} C_{XY}b\right] = \lambda C_{YY}b \\
C_{XY}^T C_{XX}^{-1} C_{XY}b = \lambda^2 C_{YY}b \\
C_{YY}^{-1} C_{XY}^T C_{XX}^{-1} C_{XY}b = \lambda^2 b \\
C_{YY}^{-1} C_{XY}^T C_{XX}^{-1} C_{XY}b - \lambda^2 b = 0
\end{gathered} \tag{12.19}$$

In an analogous way, by clearing vector b from Eq. (12.18) to substitute in Eq. (12.17), we obtain

$$C_{XX}^{-1}C_{XY}C_{YY}^{-1}C_{XY}^{T}a - \lambda^2 a = 0 \tag{12.20}$$

The solution of Eqs. (12.19) and (12.20) makes it possible to obtain the vectors a and b that represent the eigenvectors.

Once the two eigenvectors are defined, the value of their structure coefficient (r) is defined for C_{XY}, setting the option to define triple solutions according to the number of eigenvectors, that is, solutions from each eigenvector studied and their respective weight vectors (λ_i, a_i, b_i). Based on this, the canonical solutions are proposed by using the eigenvector in turn and the corresponding canonical variables (λ_i, V_i, W_i). Consequently, $\lambda_i = \text{corr}(V_i, W_i)$.

12.2.2 Satellite Images

The characteristics of the digital satellite images used correspond to the Geostationary Operational Environmental Satellite GOES-13 with coverage of the Mexican territory. The satellite GOES-13 is able to capture images of the channels of water vapor, infrared and visible available every 15 min at a temporal frequency (Meza et al. 2014) in a raw and colorless format.

The images have a .pcx extension with a BZ2 compression and tagged with a nomenclature including the date and time when they were taken, e.g., the image 201409150015.pcx corresponds to the image captured on 15 September 2014 at 00 h15 m (Meza et al. 2014).

The images as far as year 2003 have such assigned reference, in their upper left-hand corner the coordinate latitude 36.4768° and −122.2590° longitude, while their lower right-hand corner the coordinate latitude 14.1118° and longitude −79.0817°.

Since 2010, the images have a resolution of 2.36 km, with 817 pixels of latitudinal resolution and 1280 pixels of longitudinal resolution – every single one with eight bits resolution. Regarding their infrared spectrum, the images have brightness values ranging in value from 0 to 255, also known as their digital level, while the water vapor images range from digital level from 113 to 255.

12.2.3 Reading of Brightness

The temporal and spatial evolution of weather phenomena are recorded in the magnitude of the brightness value in each of the pixels that are part of the captured satellite images. The GOES-13 images used have 1,045,760 pixels, their interpretation and segmentation by threshold was made using the Sat Viewer® tool developed at the Water Research Center (CIAQ) of the Autonomous University of Querétaro (UAQ). The tool mentioned consists of a display screen for bmp format using a selection tool that generates a table of referenced brightness with nomenclature Bi, j for its identification; the subscript i corresponds to the column and j corresponds to the row of location of the pixel.

The measurements made on the interested pixels are extracted in a text file with extension .txt, which allows to calculate the temperature at the top of the clouds and make forecasts of the intensity of rain.

12.2.4 Disaggregation of Satellite Images

The characteristic features of recording and measuring instruments often present limitations for the appropriate use and comparison of information associated with weather phenomena. As previously mentioned in Sect. 12.2.2, digital images from GOES-13 have a 15-min time resolution, while the records from automatic weather stations in Mexico are 10 min long. This difference in temporal resolution required the disaggregation of the information obtained by the satellite.

This methodology is based on standardizing and normalizing the data series that come from the interpretation of the satellite images. For this purpose, first the statistical data of the series are defined, then the standardization is performed by subtracting the mean value from each of the data of the series and finally the standardization is obtained by dividing each of the results by the standard deviation. With the described operations, all the data of the series present value in the range of -1 to 1. The resulting series is characterized by a mean value equal to zero and a standard deviation with a value equal to 1.

The new series are used to determine the values that correspond to the 10-min time resolution, to be able to match both sources of information. However, this treatment is only applied to data greater than zero. Once the required values have been determined, the first step is to make an inverse process to eliminate the standardization of data based on the statistics of the series defined at the beginning of the process.

The hydro-estimator technique represents a law of regression of the estimated rain intensity with respect to the maximum temperature of the clouds. This technique requires corrections for humidity, growth and temperature gradient at the top of the clouds, to improve the estimations made (Vicente et al. 1998); this technique considers a vertical path of precipitation from the cloud to the surface where it is measured.

$$R = 1.1183x10^{11} \exp\left(-3.6382x10^{-2} T^{1.2}\right) \tag{12.21}$$

$$\mathrm{IF\,B} > 176\,\mathrm{then\,T} = 418 - \mathrm{B}$$

$$\mathrm{If\ B} \leq 176\ \mathrm{then\ T} = 330 - (\mathrm{B}/2)$$

R is the intensity predicted in mm per hour, and T is the temperature at the top of the clouds measured in degrees Kelvin (195° K to 260° K) as a function of the brightness of the pixel (B).

12.3 Evolution of the Capacities of the Dams

The National Water Commission publishes the daily volumes of each of the dams in Mexico. Although it does not constitute the official policy of the dam, it is only applied by the authorities based on experience, and the historical records represent the temporal evolution of the filling and handling of the dam. Tables 12.1 and 12.2 show an example of the evolution of the capacities of the main dams in the states of Guerrero and Michoacán.

Table 12.1 Evolution of the capacities of the dams in Michoacán state in hm^3

Dam	20/10/2015	21/10/2015	22/10/2015	23/10/2015	24/10/2015	25/10/2015
Agostitlan	16.26	16.24	16.24	16.24	16.24	16.24
Aristeo Mercado	11.99	11.99	11.99	11.92	12.22	12.38
Coíntzio	77.62	77.62	77.62	77.62	77.16	78.68
De Gonzalo	5.6	5.68	5.77	5.95	6.26	6.4
El Bosque	199.99	199.87	200	200.22	200.68	200.68
Infiernillo	5557.07	5548.79	5562.59	5609.49	5755.72	6015.06
Jaripo	9.78	9.78	9.78	9.82	10.84	10.49
Los Olivos	5.93	5.88	5.88	5.84	11.95	11.03
Melchor Ocampo	209.57	209.57	209.36	209.36	209.79	210
Pucuato	9.75	9.69	9.69	9.69	9.69	9.69
San Juanico	57.72	57.72	57.6	57.97	61.82	61.82
Tepuxtepec	420.46	420.06	419.65	419.24	418.43	418.02
Zicuiran	35.65	35.65	35.61	35.85	37.07	36.9

Table 12.2 Evolution of the capacities of the dams in Guerrero state in hm^3

Dam	20/10/2015	21/10/2015	22/10/2015	23/10/2015	24/10/2015	25/10/2015
Andres Figueroa	102.81	102.76	102.72	102.76	102.94	103.95
El Gallo	389.23	388.25	388.25	388.25	390.21	396.02
Ing. Carlos Ramirez Ulloa	1421.35	1425.89	1414.10	1398.49	1388.00	1393.46
La Calera	9.8	9.84	9.91	10.36	10.66	17.91
Revolucion Mexicana	107.38	107.38	107.86	108.07	108.35	108.28
Valerio Trujano	25.73	25.67	25.56	25.44	25.33	25.28
Vicente Guerrero	249.5	249.3	249.2	249.2	249.2	249.2

12.4 Methodology

To carry out the temporal analysis of the meteorological variables, we proceeded to identify the satellite images that coincide with the study period on 1–16 June 2012. They were decompressed, converted to bmp format and, through the application Sat-Viewer®, the brightness value of the coordinate pixel georeferenced was extracted in each of them for the principal dams along the Pacific Coast (Table 12.3, and Figs. 12.1 and 12.2). Later, the cold cloud-top temperature was determined to estimate the precipitation based on the hydro-estimator.

Once the dams under study have been located, the hurricane to be studied is selected—in this case Hurricane Carlotta, which started on 13 June 2012 and ended on 16 June 2012. The trajectory of this hurricane is shown in Fig. 12.3. Next, the hydro-estimator is applied to each of the satellite images, from which the precipitation intensity R is obtained, in mm/h. Table 12.4 shows the proposed intervals for the

Table 12.3 Location of the study dams in a satellite image whose size is 1280 x 817 pixels

State	Dam	Longitude	Latitude	1280 x 817	
				x	y
Guerrero	Ing. Carlos Ramírez Ulloa	−99.995	17.948	418	154
Guerrero	Valerio Trujano	−99.466	18.296	440	169
Michoacán	Infiernillo	−101.893	18.272	349	166
Michoacán	Tepuxtepec	−100.229	20.001	423	239

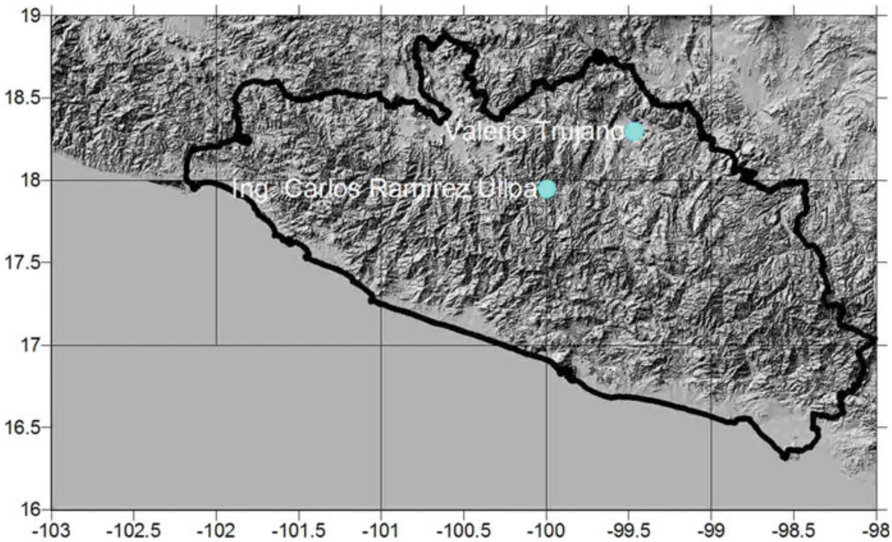

Fig. 12.1 Location map of the Carlos Ramirez Ulloa and Valerio Trujano dams in Guerrero State

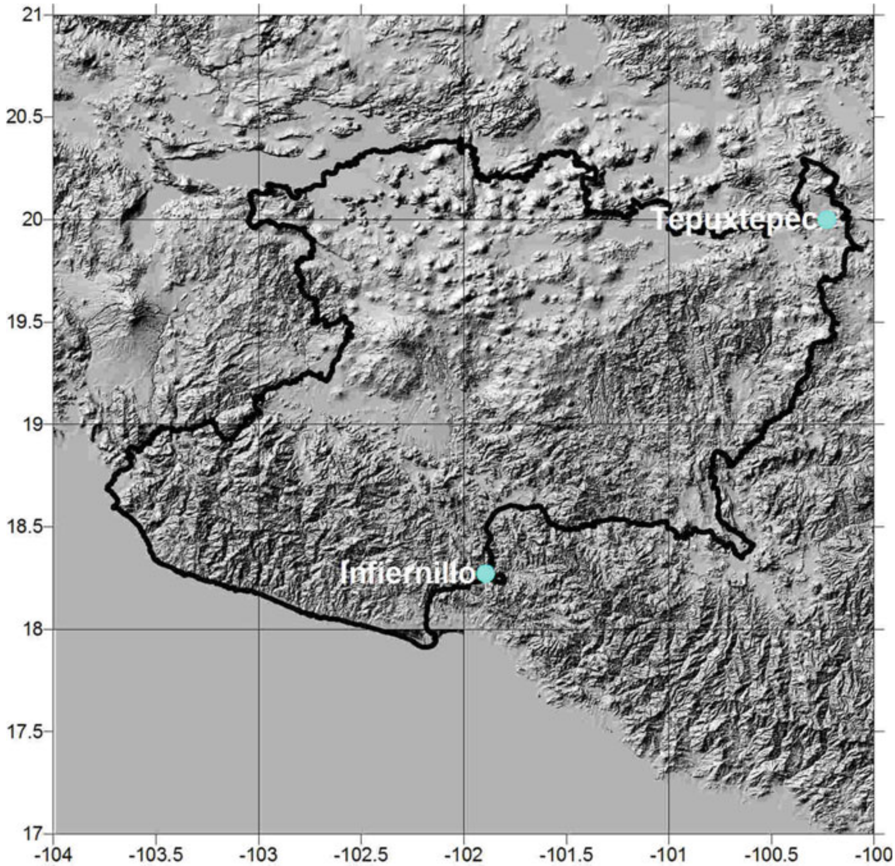

Fig. 12.2 Location map of the Infiernillo and Tepuxtepec dams in Michoacán State

intensity values obtained from the hydro-estimator. This activity makes it possible to obtain images of the hurricane's precipitation potential by adding colors.

Relevant to the policy of operation of the dams, there is access to information on the evolution of the storage of the reservoir during the entire period of occurrence of the hurricane, as shown in Table 12.3. With the data of the evolution of the precipitation obtained with Eq. (12.21), we made a data matrix, where the evolution variables of the hurricane are correlated with the evolution of the storage volume of the dam. To characterize the hurricane, we use data on the latitude and longitude of displacement of the hurricane and the velocity and atmospheric pressure in the eye. To characterize the satellite images, we use the areas of influence by counting the number of pixels in each of the proposed intervals. Finally, a canonical analysis of all

Fig. 12.3 Track of Hurricane Carlotta

Table 12.4 Scale of rainfall intensities proposed for Eq. (12.21)

Scale	Geometric area	Brightness digital level	rainfall intensities mm/h
Light blue	Z6	100–125	0.002–0.013
Blue	Z5	126–150	0.014–0.070
Green	Z4	151–175	0.075–0.362
Yellow	Z3	176–200	0.386–8.649
Orange	Z2	201–225	9.832–205.123
Red	Z1	226–235	greater than 200

Vicente et al. (1998)

the variables is carried out to forecast the evolution of the volumes of the dam and to have a tool to infer the future operation policy. In this case, the data of the first 48 h of the hurricane's evolution are used, and with the canonical analysis, the final 12 h were predicted in the hurricane's passage.

12.5 Results

With the proposed methodology, a canonical analysis of two dams in the state of Guerrero and two dams in the state of Michoacán was carried out, with the results as shown in Table 12.5. Figures 12.4, 12.5, 12.6, 12.7 show the development of Hurricane Carlotta and its respective precipitation-intensity scales. It is important to mention that estimates of the precipitation intensities were made, beginning with the onset of the hurricane's impact on the Mexican coast and up to the cessation of destruction. During this time, the storage volume variation is related canonically to the parameters of movement and the severity of the hurricane. Through the proposed methodology, we sought to forecast the dams' storage during the last moments of the hurricane. This technique enables formulating a prognostic equation correlating the evolution of the storage of the dam and the severity of the rains caused by the hurricane.

12.6 Conclusions

The results of the forecast for the operation policy of the two dams show that the canonical analysis is a reliable tool for prognosis with multivariate and multiscale variables. The results show that the correlation between the variables is greater than 90%. Figure 12.8 shows that the last 12 h of forecast are very similar to the actual capacities recorded in the dam during the passage of Hurricane Carlotta. The proposed methodology enables formulating forecast equations based on historical data that can describe the behavior of the dam capacities during the passage of a hurricane.

Table 12.5 Evolution of the capacities of the dams in Guerrero state in hm^3

State	Dam	Capacities (hm^3)			
		June 13th	June 14th	June 15th	June 16th
Guerrero	Ramirez Ulloa	1012.6	989.6	987.2	969.3
Guerrero	Valerio Trujano	11.91	11.84	11.8	11.77
Michoacán	Tepuxtepec	283.28	283.28	282.84	282.94
Michoacán	Infiernillo	2817.94	2817.94	2827.65	2872.65

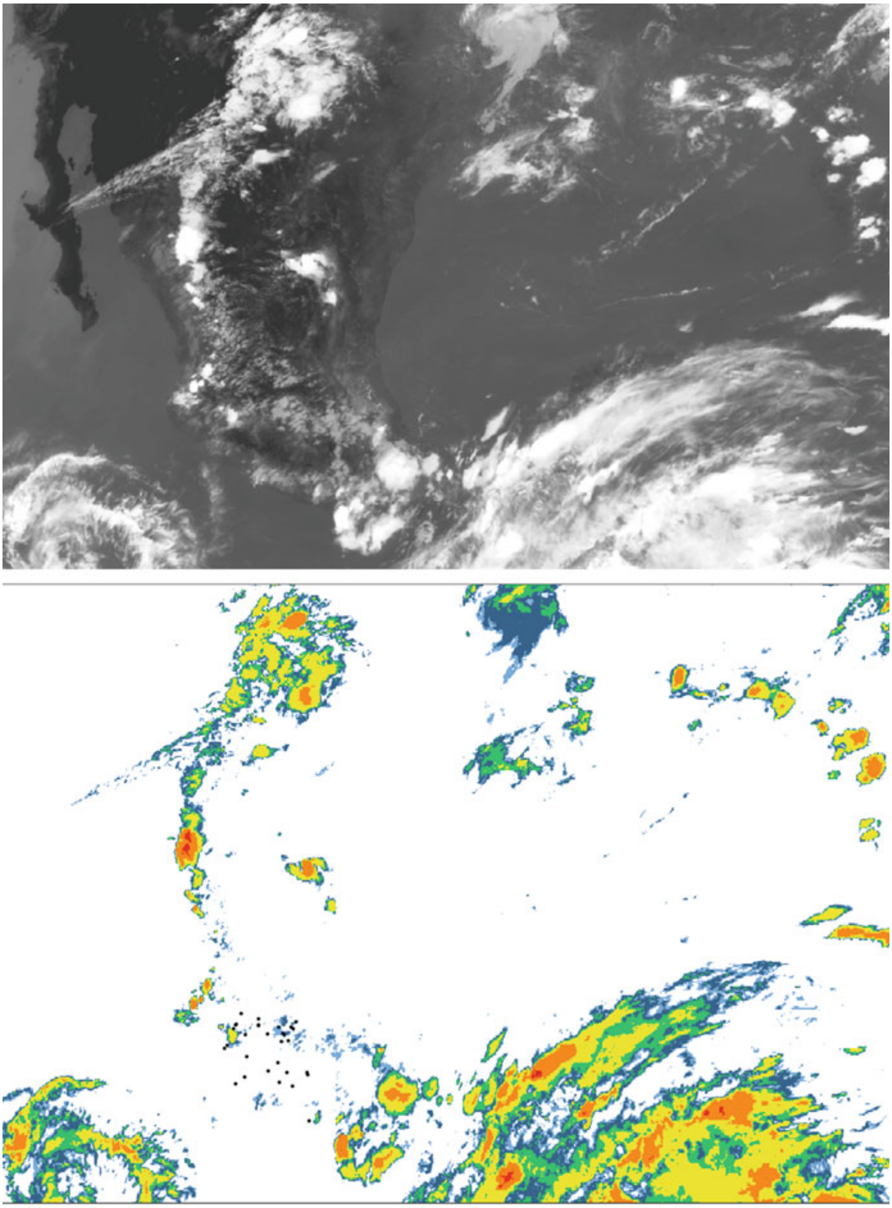

Fig. 12.4 Image and track of Hurricane Carlotta 201206132201

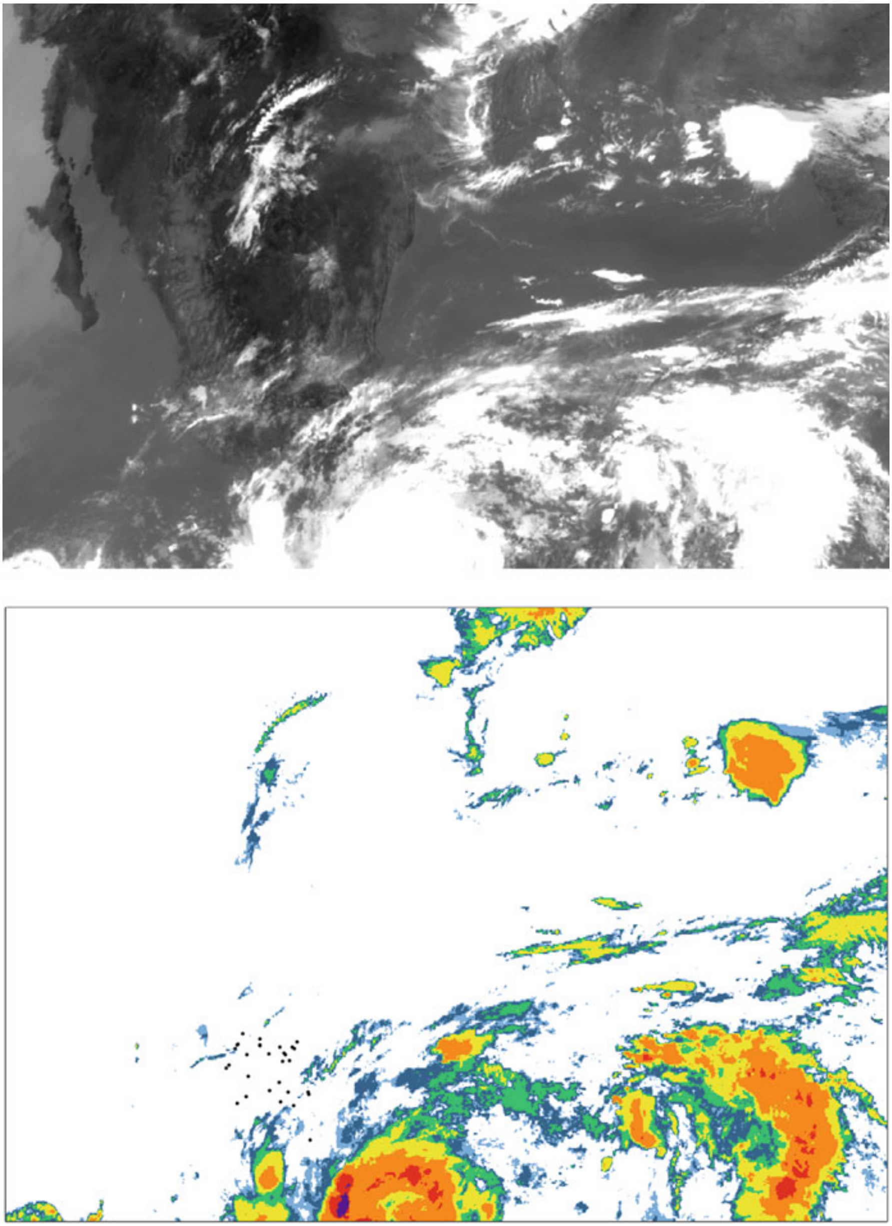

Fig. 12.5 Image and track of Hurricane Carlotta 201206151601

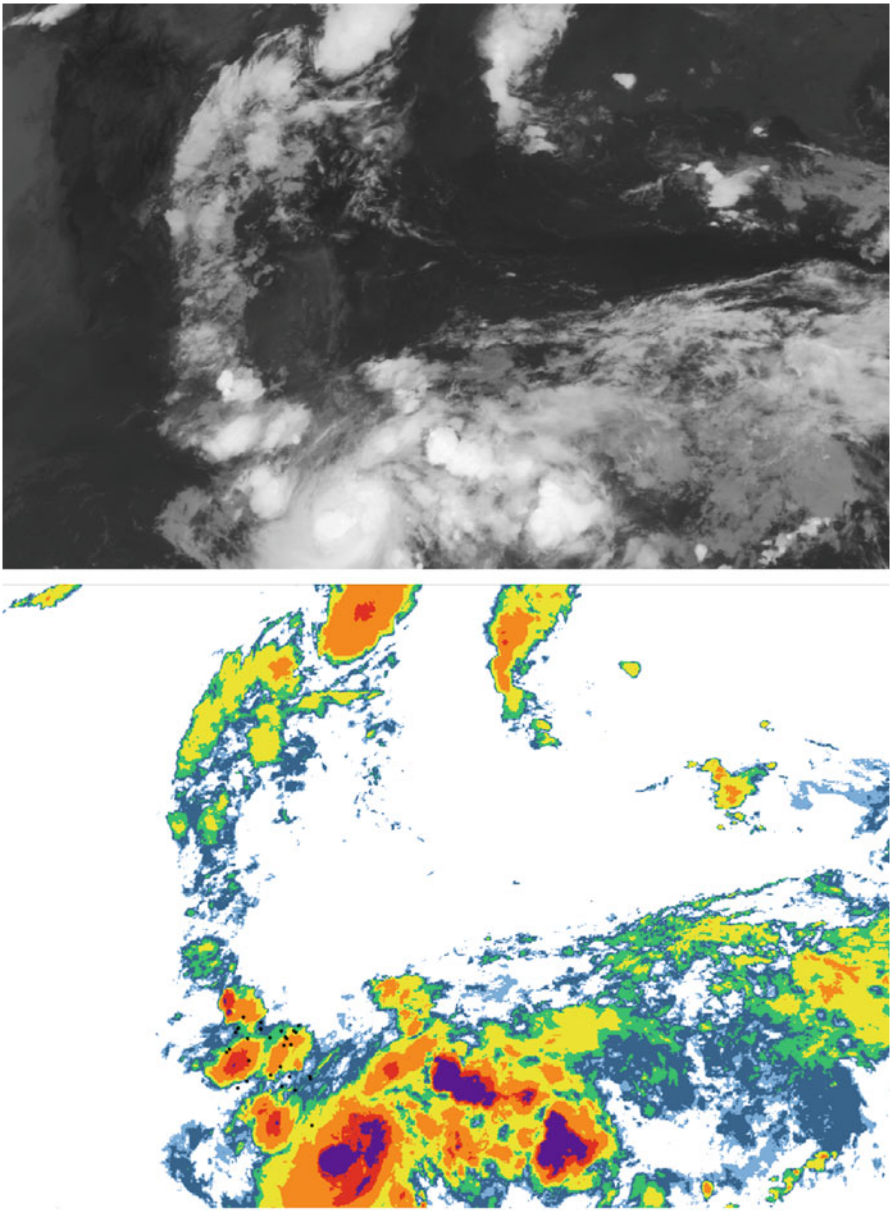

Fig. 12.6 Image and track of Hurricane Carlotta 201206160401

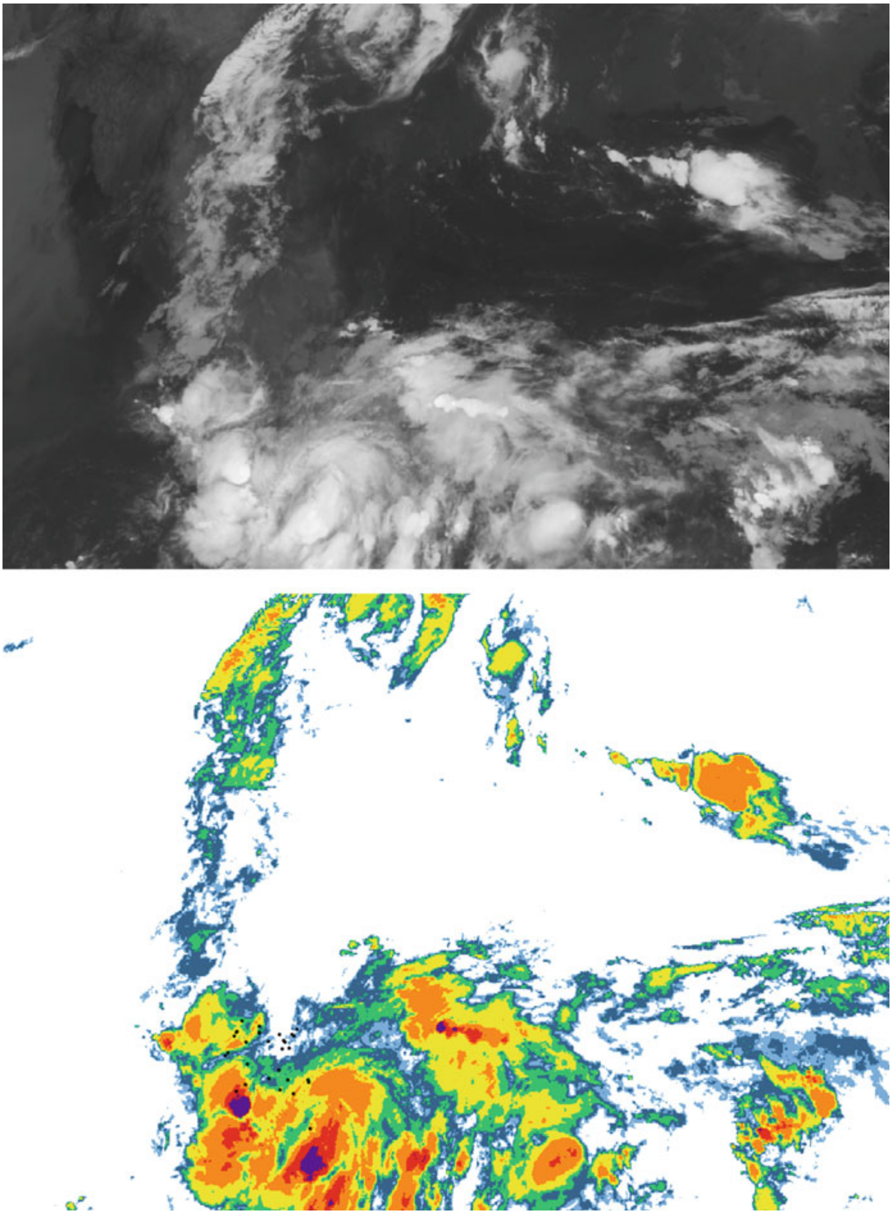

Fig. 12.7 Image and track of Hurricane Carlotta 201206161001

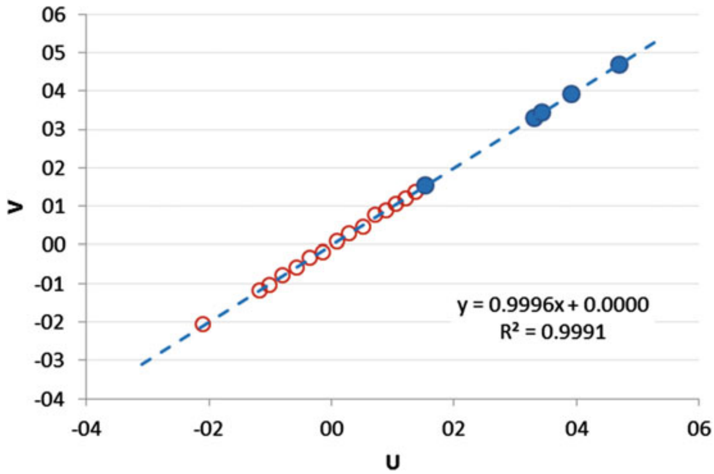

Fig. 12.8 Dams operation policy of Valerio Trujano dam

References

Albanil EA, Pascual RR, López QM, Quiroz AC, Chablé PLA (2015) Annual report 2015. Summit report in Mexico. General Coordination of the National Meteorological Service. Meteorology and Climatology Management. Sub management of Forecast to Medium and Long Term

Andenberg MR (1973) Cluster analysis for applications. Academic Press, New York

Beran MA, Brilly M, Becker A, Bonacci O (1990) Regionalization in hydrology, IAHS Publication no. 191. International Association of Hydrological Sciences, Wallingford, p 260

Brown P, Russell B (2001) Siting and maintenance of weather stations. Turf irrigation management series: III. College of Agriculture and Life Sciences. The University of Arizona

Closas AH, Arriola EA, Kuc CI, Yellow MR, Jovanovich EC (2013) Multivariate analysis, concepts and applications in Educational Psychology and Psychometrics. Approaches vol. 25 no.1 Libertador San Martín jun

Crespin EEO (2016) Análisismultivariante: aplicaciones con SPSS, 1st edn. UFG Editores, San Salvador, 304 p

De la Fuente FS (2011) Conglomerate analysis. Faculty of Economics and Business Sciences. Autonomous University of Madrid

Garcia-Osorio C, Fyfe C (2005) Visualization of high-dimensional data via orthogonal curves. J Univ Comput Sci 11(11):1806–1819

Hair JF, Anderson RE, Tatham RL, Black W (2009) Multivariate data analysis, 7th edn. Prentice Hall, Englewood Cliffs

Jolliffe IT (2002) Main component analysis, 2nd edn. Springer, New York, p 487

Medina GG, Grangeda GJ, Ruiz CJA, Báez G (2008) Use of meteorological stations in agriculture. Information brochure 50. National Institute of Forestry, Agriculture and Livestock Research. http://www.zacatecas.inifap.gob.mx/publicaciones/Uso_de_estaciones_meteorologicas_en_la_agricultura.pdf. Accessed 27 February 2017

Meza RM, Curiel HL, González TDME, Álvarez MC (2014) Satellite images and spatial distribution of rainfall in the state of Querétaro. Case: Storm of August 18, 2014. University network for characterization of hydrometeorological, fluvial and coastal risks. Nthe. Electrical magazine of scientific, technological and information dissemination of the state of Querétaro. Periodicity: quarterly—2016 No.14.

National Water Commission (CNA) (2012) National Meteorological Service: 135 years of history in Mexico. http://www.conagua.gob.mx/CONAGUA07/Publicaciones/Publicaciones/CGSMN-1-12.pdf. Accessed 3 March 2017

Prieto GRE (2006) Classification statistical techniques. An example of Cluster analysis. Monograph to obtain the title of Industrial Engineer. Institute of Basic Sciences and Engineering. Autonomous University of the State of Hidalgo

Vicente GA, Scofield RA, Menzel WP (1998) The operational GOES infrared rainfall estimation technique. Bull Am Meteorol Soc 79:1883–1898

Wilks DS (2006) Statistical methods in the atmospheric sciences, International geophysics series, 2nd edn. Academic Press, Amsterdam